IET Nanobiotechnology

Research Article

IET Journals
The Institution of Engineering and Technology

Synthesis, physicochemical characterisation and biological activity of anandamide/ε-polycaprolactone nanoparticles obtained by electrospraying

ISSN 1751-8741
Received on 6th March 2019
Revised 3rd October 2019
Accepted on 13th November 2019
doi: 10.1049/iet-nbt.2019.0108
www.ietdl.org

Virna M. Martín Giménez[1], Marcos G. Russo[2,3], Griselda E. Narda[2,3], Lucía B. Fuentes[4], Luciana Mazzei[5,6], Carlos Gamarra-Luques[5], Diego E. Kassuha[1], Walter Manucha[5,6] ✉

[1]Instituto de Investigaciones en Ciencias Químicas, Facultad de Ciencias Químicas y Tecnológicas, Universidad Católica de Cuyo, Av. Ignacio de la Roza 1516 (o), 5400, San Juan, Argentina

[2]Instituto de Investigación en Tecnología Química, INTEQUI, CONICET, San Luis, Argentina

[3]Departamento de Química, Facultad de Química, Bioquímica y Farmacia, Universidad Nacional de San Luis, Almirante Brown 1455, D5700HGC, San Luis, Argentina

[4]Facultad de Química, Bioquímica y Farmacia, Universidad Nacional de San Luis, Chacabuco 917, D5700HOJ, San Luis, Argentina

[5]Instituto de Medicina y Biología Experimental de Cuyo, Consejo Nacional de Investigación Científica y Tecnológica (IMBECU-CONICET), Av. Ruiz Leal s/n – Parque Gral. San Martín, M5500 Mendoza, Argentina

[6]Laboratorio de Farmacología Experimental Básica y Traslacional. Área de Farmacología, Departamento de Patología, Facultad de Ciencias Médicas, Universidad Nacional de Cuyo, Av. Libertador 80 – Parque General San Martín, Centro Universitario, M5500 Mendoza, Argentina

✉ *E-mail: wmanucha@yahoo.com.ar*

Abstract: Drug encapsulation in nanocarriers such as polymeric nanoparticles (Nps) may help to overcome the limitations associated with cannabinoids. In this study, the authors' work aimed to highlight the use of electrospraying techniques for the development of carrier Nps of anandamide (AEA), an endocannabinoid with attractive pharmacological effects but underestimated due to its unfavourable physicochemical and pharmacokinetic properties added to its undesirable effects at the level of the central nervous system. The authors characterised physicochemically and evaluated in vitro biological activity of anandamide/ε-polycaprolactone nanoparticles (Nps-AEA/PCL) obtained by electrospraying in epithelial cells of the human proximal tubule (HK2), to prove the utility of this method and to validate the biological effect of Nps-AEA/PCL. They obtained particles from 100 to 900 nm of diameter with a predominance of 200–400 nm. Their zeta potential was −20 ± 1.86 mV. They demonstrated the stable encapsulation of AEA in Nps-AEA/PCL, as well as its dose-dependent capacity to induce the expression of iNOS and NO levels and to decrease the Na^+/K^+ ATPase activity in HK2 cells. Obtaining Nps-AEA/PCL by electrospraying would represent a promising methodology for a novel AEA pharmaceutical formulation development with optimal physicochemical properties, physical stability and biological activity on HK2 cells.

1 Introduction

Cannabinoids and their derivatives – both natural and synthetic origin –, represent an interesting therapeutic potential in cardiovascular diseases such as arterial hypertension, also as antiemetic and stimulants of appetite in debilitating diseases, analgesics for the treatment of multiple sclerosis and cancer, among other pathologies. However, despite its high clinical potential, only some dosage forms are currently available due to their unfavourable physicochemical and pharmacokinetic properties added to the undesirable effects at the level of the central nervous system associated with these therapies [1–4].

In this paper, medicine uses nanotechnology to direct specifically the active ingredients towards their therapeutic target, avoiding or reducing their side effects, increasing their solubility, prolonging their release, as well as preventing their chemical, photochemical, or oxidative degradation [5–7]. In this regard, several authors have conducted research aimed at developing and optimising various nanosystems for the administration of cannabinoids for pharmaceutical use through the production of micro and nanoparticles of lipid and polymeric nature [8, 9]. These nanosystems have been shown to encapsulate the mentioned active principles effectively, achieving an increase in their solubility and stability, improving their absorption, protecting them from premature enzymatic degradation or metabolism in the body, prolonging their circulation time and limiting their side effects [5, 10].

Of particular interest, an article that examined the potential of nanoparticles administered by inhalation to treat lung cancer demonstrated that its use would provide a promising strategy for overcoming the current clinical limitations of the unwanted psychoactive effects of cannabinoids used in the treatment of this type of tumours [1]. Similarly, some studies have demonstrated an intense anticancer activity of the PEGylated and non-PEGylated polymeric micro and nanoparticles, loaded with the phytocannabinoid Δ(9)-tetrahydrocannabinol in lung cancer and others [2, 3, 11–13]. Other scientific works reported that the synthetic cannabinoid CB13 (which as a consequence of its poor solubility in gastrointestinal fluids is not entirely absorbed orally) encapsulated in nanoparticles of polylactic-co-glycolic acid coated with polyethylene glycol [14, 15], showed a remarkable analgesic efficacy with a very prolonged pain relief effect that lasted up to eleven days after the administration of an oral dose compared to free CB13 [16]. It was also shown the development of WIN nanomicelles (synthetic cannabinoid with potent anticancer effects) conjugated with maleic styrene acid reduces side effects and increases the efficacy of the drug [17]. Similar results were found when analysing the antitumour activity of cannabidiol released from microparticles of epsilon polycaprolactone (PCL) showing potential therapeutic advantages over the free drug [3].

In the particular case of the endocannabinoid anandamide (AEA), it has been reported that its incorporation into spherical PCL nanoparticles provided chemical stability for AEA in contact with plastic materials and when stored as a liquid suspension in the

dark. The strong affinity of the drug for the polymer showed a prolonged passive diffusion rate of AEA through an artificial model of lipid membrane [18]. Similarly, this same type of nanoparticle was used to evaluate the existence of a membrane transporter that regulates the extracellular levels of AEA, demonstrating that the cellular uptake of AEA encapsulated in PCL became much less sensitive to the inhibitors of the specific transporter [19]. In both studies, the Nps-AEA/PCL was obtained by nanoprecipitation. The use of the nanoprecipitation method is not recommended for the loading of highly hydrolysable and thermolabile drugs because it is a technique that consists of several steps that include obtaining of particles in an aqueous medium and subsequent drying stage, which makes it a particular, tedious and lengthy procedure [20].

In relation to the aforementioned endocannabinoid and its renal effects, a study carried out by Silva *et al.* reported that AEA was able to increase the concentration of nitric oxide (NO) in cells of the thick ascending limb of the loop of Henle through the activation of cannabinoid receptor type 1 (CB1) receptors and the subsequent signalling of the NO synthase (NOS) enzyme. The NO produced would cause blockage of apical channels that carry sodium in these cells, favouring its excretion as well as diuresis [21]. Likewise, it has been demonstrated that renal epithelial cells of the human proximal tubule (HK2) express the CB1 receptor [22]. Additionally, it was also shown that the Na^+/K^+ ATPase pump presents in the basolateral membrane of the renal proximal tubular epithelium is one of the essential transporters responsible for maintaining the volume and composition of extracellular fluid through different signalling pathways [23].

Therefore, based on the background above, our laboratory proposed as central objectives of the present work: first, to synthesise polymeric nanoparticles carrying AEA (Nps-AEA/PCL) by electrospraying technique. Second, to characterise them regarding their main physicochemical properties; and, finally, to evaluate their biological activity in HK2 cell cultures through the measure of their ability to enhance the inducible isoform of NOS (iNOS) expression and the determination of NO levels and their impact over the Na^+/K^+ ATPase activity.

2 Materials and methods

2.1 Materials

ε-PCL was donated by the Instituto de Investigaciones en Ciencia y Tecnología de Materiales (INTEMA-CONICET-UNMdP). AEA brand Cayman Chemical (Michigan, USA) and quality pro-analysis acetone from Laboratorios Cicarelli (Santa Fe, Argentina), were utilised. Moreover, we used an infusion pump for syringes brand KD Scientific, a high-voltage electric source (0–30 kV) brand Gamma High Voltage Research, a glass syringe (to avoid corrosion by the solvent) of 20 ml with diameter internal of 20 mm, a metal needle and a metal collector plate covered with aluminium foil.

2.2 Preparation of PCL-nanoparticles charged with AEA

A 0.5% w/w solution of PCL in acetone was prepared. After the complete dissolution of PCL, 5 mg of AEA was added. A glass syringe was charged with the polymer solution prepared as described above and mounted on the infusion pump. The pump was programmed to a flow of 0.5 ml h^{-1}, and an inner diameter of 20 mm syringe. The needle-collector distance was 15 cm. The voltage used was 10 kV. The particles were removed from the collector with the help of a silicone spatula.

2.3 Spectroscopic characterisation by infrared spectroscopy by Fourier transform (FTIR)

The FTIR spectra were recorded with a Nicolet Protégé 460 spectrometer, in the range of 4000–225 cm^{-1}, with 64 scans and spectral resolution of 4 cm^{-1}. For the preparation of the pellets (PCL and Nps-AEA/PCL), KBr was used as a spectroscopic quality diluent, melted and then stored in an oven. The spectrum of the AEA was collected from the commercial ethanolic solution of the endocannabinoid using ZnSe windows.

2.4 Spectroscopic characterisation by UV–visible (UV–vis) spectroscopy

The UV–vis absorption spectra of AEA and Nps-AEA/PCL in ethanol were measured in quartz cells (optical path = 10 mm) in a Shimadzu UV-160 spectrophotometer, equipped with a CPS-240A cell positioner; the temperature was controlled at 25 ± 0.1°C.

2.5 Thermogravimetric analysis (TGA)

The TG curves were recorded on a Shimadzu TGA-51 instrument from room temperature to 300°C, with 50 ml min^{-1} of nitrogen flow and a heating rate of 5°C min^{-1}. The samples were appropriately placed in platinum cells.

2.6 Differential scanning calorimetry (DSC)

The DSC curves were recorded on Shimadzu DSC-60 equipment from room temperature to 300°C under nitrogen atmosphere flowing at 50 ml min^{-1}, with a heating rate of 5°C min^{-1}. PCL and Nps-AEA/PCL were placed in open aluminium cells, while for AEA, aluminium cells with perforated lid were used; in both cases, an empty aluminium cell was used as a reference. The melting temperature was determined as the peak of the process.

2.7 Scanning electron microscopy (SEM)

The SEM images were recorded to determine the morphology and size of the Nps-AEA/PCL using a LEO1450DP microscope. The sample was directly observed on the aluminium foil in which it was collected, to which a gold cover was applied. The analysis of the images obtained was carried out using ImageJ version 1.x image processing software.

2.8 Dynamic light scattering (DLS)

DLS assessed the zeta potential as a measure of the surface charge of the particles. It was determined at room temperature in a Zetasizer® 3000HS (Malvern Instruments, UK). 1 mg dried Nps was suspended in 1 ml of distilled water before measurement. The analysis was carried out in triplicates.

2.9 Physical stability tests

In order to evaluate the physical stability of the Nps-AEA/PCL at different temperatures, they were subjected to three different temperature values (4, 25 and 40°C) during a period of four months. The samples were analysed by FTIR at 30, 60 and 120 days in order to determine their physical stability.

2.10 Cell line and culture conditions

Human renal tubular epithelial HK2 (ATCC® Number: CRL-2190™) were maintained in Dulbecco`s Modified Eagle Media (DMEM, GIBCO®, Grand Island, NY, USA) and supplemented with 10% foetal bovine serum (Internegocios®, Mercedes, Buenos Aires, Argentina), 100 µg/ml streptomycin and 100 U/ml penicillin (GIBCO®, Grand Island, NY, USA) at 37°C in a humidified atmosphere with 5% CO_2.

2.11 Cells treatment

To perform the cellular protocol, 1×10^6 HK2 cells were seeded in Petrís dishes (100 mm diameter, Biofil®, Argentina). After 24 h, the supernatant was aspirated and the media was replaced with the appropriate treatments: free AEA, was used at 1 and 10 µM; Nps-AEA/PCL with encapsulated AEA was added to reach 1 and 10 µM of AEA; PCL alone was added at 141 µg/ml (maximum concentration reached when AEA was 10 µM) and; finally, the control group did not receive any treatment. In the three treated groups, AEA and nanoparticles were dissolved in control media.

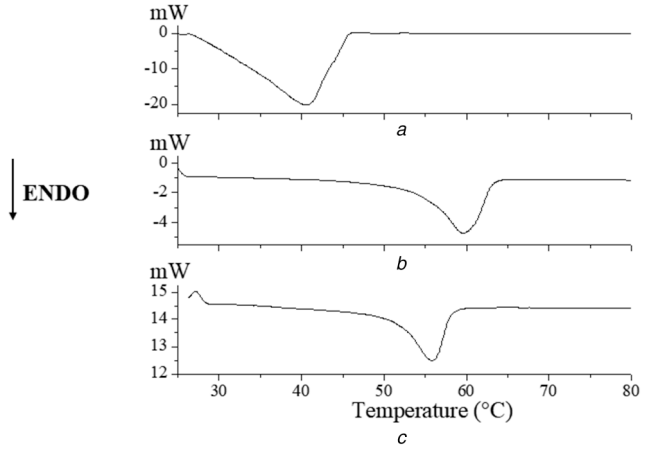

Fig. 1 *DSC curves of*
(a) AEA, ***(b)*** PCL, ***(c)*** Nps-AEA/PCL

The treatments were performed for 24 h; then, cells were scrapped, pelleted, washed with saline phosphate buffer (PBS) and stored at −80°C until use. All tests were performed in duplicate.

2.12 iNOS protein expression by western blot technique

The HK2 cellular lysed were homogenised, and protein levels were quantified by Bradford assay with bovine serum albumin (BSA) 10 mg/ml as a standard. Samples were prepared in sodium dodecyl sulphate (SDS) sample buffer (31.25 mM Tris-HCl, pH 6.8, 10% glycerol, 0.0025% bromophenol blue, 10 mM dithiothreitol, 1% SDS). The samples containing 20 µg of proteins were electrophoresed in SDS (0.1%) and 8% polyacrylamide gel with 4% stacking gel and then transferred to nitrocellulose. In the next step, softly removed blot from the gel and placed it in a container with 15 ml of Ponceau S protein staining solution. Immediately, we proceeded to block the non-specific binding sites with 5% non-fat dry milk in PBS plus 0.1% Tween for 1 h RT, washed and then incubated overnight in the primary antibody against iNOS (C-11 mouse monoclonal, 1:2500) from Santa Cruz Biotechnology. We used the β-actin expression as a housekeeping gene (C4, mouse monoclonal antibody, 1:1500). Detection was accomplished with secondary antibodies (DAKO). Densitometric analysis was carried out by image analysis software, and the photographs were digitalised by using a scanner (LACIE Silver Scanner for Macintosh) and the Desk Scan software (Adobe Photoshop) on a desktop computer. The immunosignal ratio was standardised to 1 for the appropriate control values (HK2 cells without treatment).

2.13 Determination of nitrite levels in HK2 cells

We measured nitrite levels by Griess reaction with minor modifications [24]. Homogenates from lizated HK2 cells were incubated with 10 mmo1/l l-Arginine in a buffer (pH 7.40) containing 25 mmol/l HEPES, 140 mmol/l NaCl, 5.4 mmol/l KCl, 1.8 mmol/l $CaCl_2$, 1 mmol/l $MgCl_2$, and 5 mmol/l glucose at 37°C for 24 h. After centrifugation at 6400 rpm for 20 min, the supernatants were used for the assay of indirect NO production and the amount was corrected by means of the protein amount, measured according to the Bradford method. Nitrites were measured by a spectrophotometer at 540 nm wavelength. The data present were expressed as nmol of nitrite generated per µg protein per 100 µl homogenate.

2.14 Assay for Na^+/K^+ ATPase activity

The ATPase activity was performed according to previous reports [25]. HK2 cells were washed and suspended in a cold solution and transferred to Eppendorf tubes. For the assay, each sample was incubated at 37°C for 15 min with the presence of 1 mmol/l adenosine 5′-triphosphate (ATP). After the incubation time, the Eppendorf tube was immersed in a boiling water bath for 5 min. The samples were centrifuged, and the free inorganic phosphate produced was determinate in the supernatant fraction using the malachite-green technique. The samples were diluted with dissection solution up to 250 µl and mixed with 1 ml of the malachite-green reagent 0.03% $Na_2MO_4{\cdot}2H_2O$, 0.02% malachite green oxalate, 0.05% Triton X-100, and 0.7 mol/l HCl. Also was added a volume of 0.1 mL sodium citrate solution (33%) to every sample. Then samples were incubated for 30 min at RT. Optical density was performed at 600 nm. The standard curve was obtained incubating 200 µl of a known phosphate concentration solution with 1 ml of malachite-green reagent.

Finally, Na^+/K^+ ATPase activity expressed as the picomole of inorganic phosphate per minute incubation was determined by quantifying the difference in inorganic phosphate released from ATP in the absence and presence of ouabain (2 mM).

2.15 MTT assay

The potential cytotoxic activity of Nps-AEA/PCL was studied by MTT [(3-(4,5-dimethylthiazol-2-yl)-2,5-diphenyl tetrasodium bromide)] assay with the aim of determining the cell viability. Briefly, upon completion of the pharmacological treatment, HK2 cells were loaded with MTT to a final concentration of 0.5 mg/ml and incubated for 4 h at 37°C. The chromogen formed was dissolved in dimethyl sulfoxide (DMSO), and the optic density value measured at 570 nm was used to index cell viability. The absorbance of the untreated HK2 cells (controls) was also estimated to calculate relative cell viability (in percentage). The assay was performed in triplicate.

For the photographic record, 150,000 cells were plated on coverslips located at the bottom of the six-well plate. After 24 h, the same treatments as explained above were applied. After 24 h, the medium was removed, two rinses were made with PBS, and the cells were fixed with methanol for 30 min. Subsequently, they were stained with crystal violet and mounted on slides.

2.16 Statistical analysis

In studies that required statistical analysis, the results were assessed by two-way analysis of variance for comparisons among groups. Differences among groups were determined by Bonferroni post-test. A $P < 0.05$ was considered to be significant. Results are given as means ± standard error medium (SEM). Statistical tests were performed by using GraphPad In Sat version 3.00 for Windows 95 (Graph Pad Software, Inc., San Diego, CA, USA).

3 Results

3.1 DSC analysis and TGA

Fig. 1 shows the DSC curves corresponding to the Nps-AEA/PCL compared to those obtained for AEA and PCL separately. Specifically, in Fig. 1*a*, corresponding to AEA, an endothermic signal is observed at 40.13°C ($\Delta Hf = 2.65$ kJ g^{-1}), which can be associated with the melting process of the endocannabinoid. The fusion process of the polymer (Fig. 1*b*) is observed at 59.60°C ($\Delta Hf = 59.59$ J g^{-1}). The DSC curve corresponding to the Nps-AEA/PCL (Fig. 1*c*) shows a single endothermic signal at 55.85°C ($\Delta Hf = 44.38$ J g^{-1}), evidencing an increase in the thermal stability of AEA in the Nps-AEA/PCL in relation to free AEA.

In addition to DSC analysis, samples of PCL and Nps-AEA/PCL were also evaluated thermogravimetrically (Fig. 2) in order to corroborate the thermal behaviour in the temperature ranges associated with the melting events observed in the DSC curves. It was not observed a significant mass loss in the temperature range corresponding to the melting processes, assigned from the DSC analysis, so it is verified that the endothermic signals of these substances can be assigned to their melting processes. TGA was not performed for the ethanoic solution of AEA.

3.2 FTIR analysis

Due to the complexity of the obtained spectra, only the vibrational modes of the main AEA and PCL functional groups potentially associated with some interaction (Figs. 3*A* (*a* and *b*), respectively)

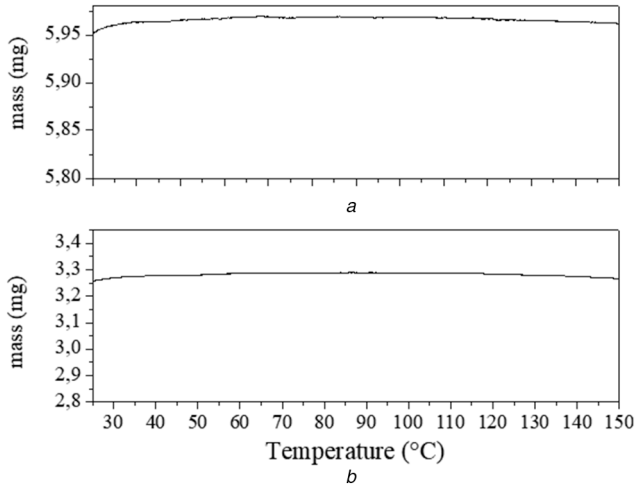

Fig. 2 *TG curves of*
(a) AEA, ***(b)*** Nps-AEA/PCL

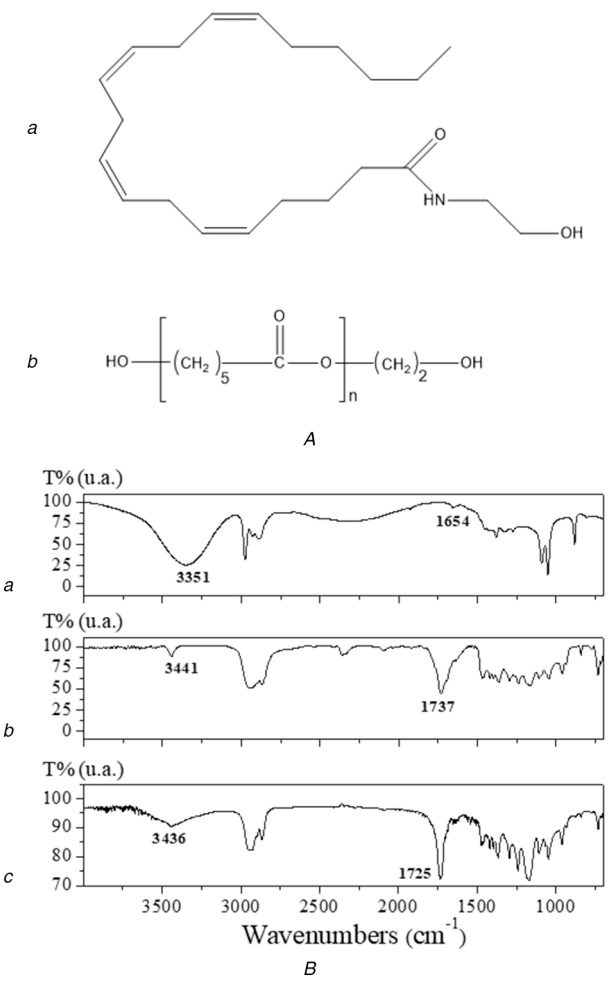

Fig. 3 *FTIR analysis*
(A) Molecular structure of (a) AEA and (b) PCL, ***(B)*** FTIR spectra of (a) AEA, (b) PCL and (c) Nps-AEA/PCL

were analysed (Fig. 3B). This study allows detecting band shifts or modifications that may be related to possible interactions between the components of the system under study.

The FTIR spectrum of AEA shows broadband at 3351 cm^{-1}, which can be assigned to υ-(O–H); with a contribution of υ-(N–H). Additionally, the weak band observed at 1654 cm^{-1} is assigned to υ-(C–=–O) involved in intra- or inter-molecular H-bond interactions justifying its position and intensity. In the spectrum of PCL, the characteristic band of υ-(O–H) is observed at 3441 cm^{-1}, while υ-(C–=–O) is observed at 1737 cm^{-1}. The FTIR analysis of

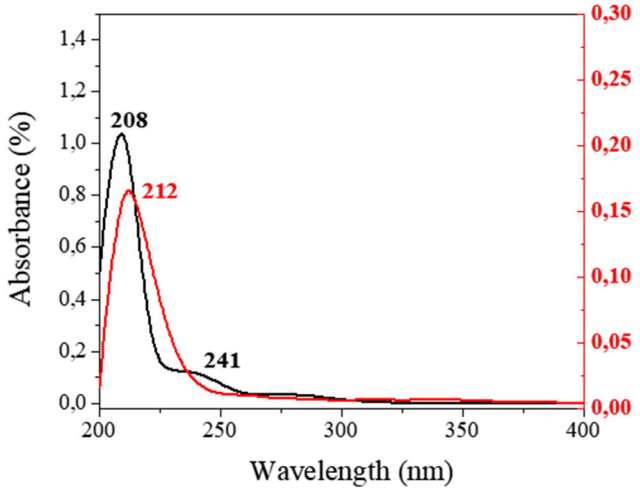

Fig. 4 *UV–vis spectra of AEA (black) and Nps-AEA/PCL (red)*

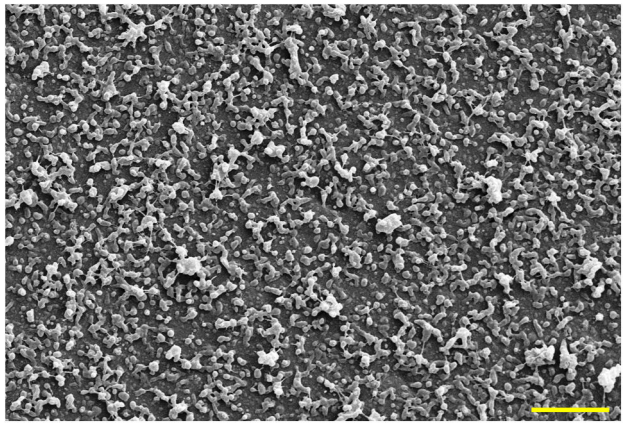

Fig. 5 *Morphology and size characterisation by SEM. Magnification 1.5 kx. Scale 10 μm*

the Nps-AEA/PCL spectrum suggests potential inter-molecular interactions between AEA and PCL. The υ-(C–=–O) vibrational mode of PCL is shifting to lower wavenumber, indicating a weakening of this bond. On the other hand, the υ-(O–H) and υ-(N–H) vibrational modes of AEA are found to higher wavenumber, due to the reinforcement of these bonds. These shiftings are probably indicative of inter-molecular H-bond interactions between AEA and PCL in the nanoparticles. The υ-(C–=–O) vibrational mode of AEA in the Nps-AEA/PCL spectrum could not be identified due to overlapping with PCL bands.

3.3 UV–vis analysis

The UV–vis spectra corresponding to AEA and Nps-AEA/PCL are shown in Fig. 4. AEA presents two absorption bands centred at 208 and 241 nm, which could be attributed to π–π* transitions. A bathochromic displacement of the band at 208 nm, the disappearance of the band at 241 nm, and a significant decrease in absorbance was observed in the UV–vis spectrum of Nps-AEA/PCL. These facts can potentially suggest that in the process of encapsulation of the endocannabinoid there are interactions between both components of the system.

3.4 SEM and DLS analysis

Fig. 5 shows the SEM microphotographs of the Nps-AEA/PCL, evidencing its spherical or ovoid and smooth surface nature. These are distributed in a range of sizes between 100 and 900 nm, the most predominant being those between 200 and 400 nm (Fig. 6), considering a population of 100 particles. Additionally, the presence of agglomerates of nanoparticles that affect the homogeneity of the sample was observed. In terms of the surface charge of the particles, their zeta potential was −20 ± 1.86 mV.

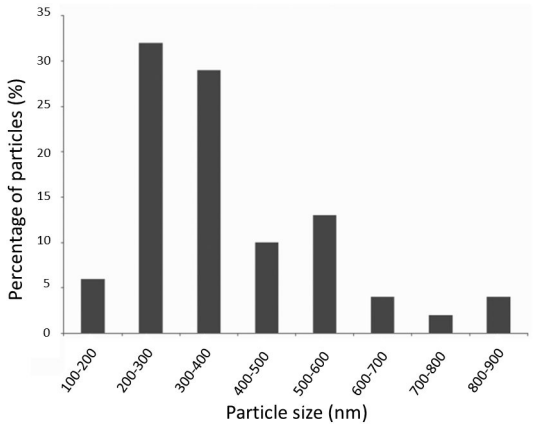

Fig. 6 *Particle size distribution of Nps-AEA/PCL considering a population of 100 particles*

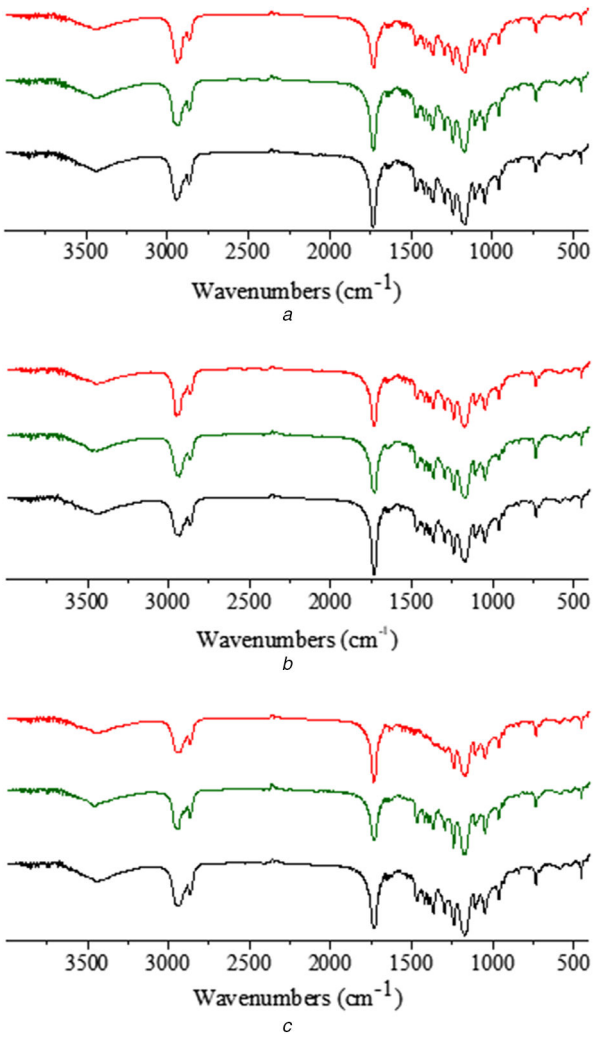

Fig. 7 *FTIR spectra of solids from physical stability assay of Nps-AEA/PCL at*
(a) 30 days, ***(b)*** 60 days, ***(c)*** 120 days. Red, green and black colours correspond to a storage temperature of the particles at 4, 25 and 40°C, respectively

3.5 Physical stability tests

The evaluation of the physical stability of the Nps-AEA/PCL was performed by storage the samples in real-time under different temperature and humidity conditions during several periods, as mentioned previously. The stability was checked by FTIR analysis (Fig. 7), confirming that the samples remained unchanged in all the conditions evaluated. This physical stability could be attributed to the intermolecular interactions between AEA and PCL described previously (see Section 3.2). In this sense, intermolecular

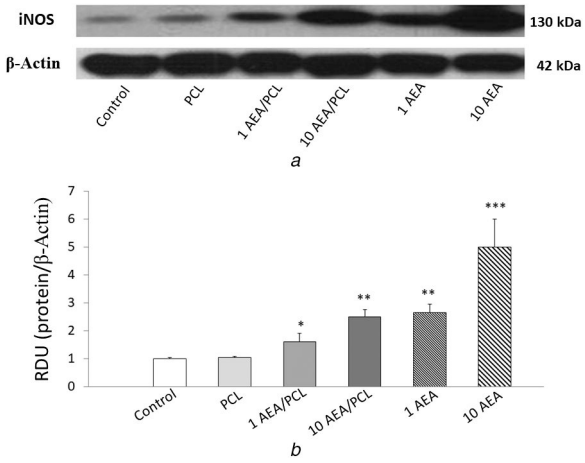

Fig. 8 *iNOS protein expression in HK2 cells by AEA treatment*
(a) Western blot, ***(b)*** Histogram

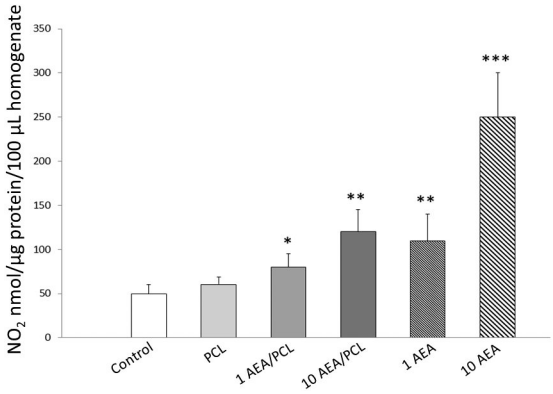

Fig. 9 *NO bioavailability in HK2 cells linked to AEA treatment*

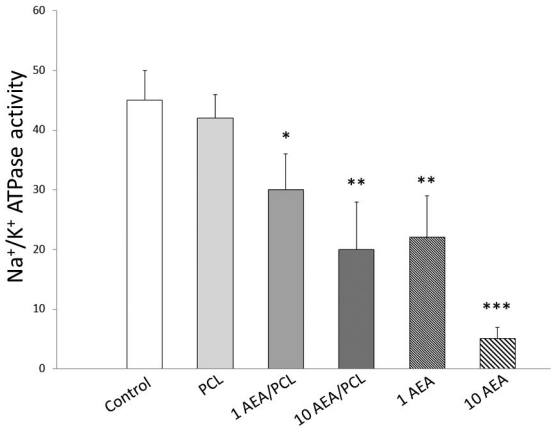

Fig. 10 *Effect of Nps-AEA/PCL on Na^+/K^+ ATPase activity in HK2 cells*

interactions have been found in other multi-component systems with PCL [26] and they are responsible for the increased thermal stability.

3.6 iNOS expression, NO levels, and Na^+/K^+ ATPase activity in HK2 cells

Figs. 8–10 show overexpression of iNOS as well an augmented production of nitrites, and a reduction in the Na^+/K^+ ATPase activity in those cells that received treatment for 24 h with AEA either encapsulated in Nps-AEA/PCL or non-encapsulated in them compared to control, in a dose-dependent manner. Control and PCL group levels were similar between them. Fig. 8 shows the bands immunostained to reveal levels of iNOS in the HK2 cells. In 1 μM concentration of AEA it was observed an iNOS expression increased with values of 1.60 ± 0.30% for Nps-AEA/PCL and 2.65

± 0.30% for free AEA versus 1.00 ± 0.03% or 1.05 ± 0.03%; P <0.05 or P <0.01 of control or PCL group, respectively. The concentration of nitrites (Fig. 9) was of 80 ± 15% for Nps-AEA/PCL and 110 ± 30% for free AEA versus 50 ± 10% or 60 ± 10%; P <0.05 or P <0.01 of control or PCL group, respectively. The Na^+/K^+ ATPase activity (Fig. 10) was of 30 ± 6% for Nps-AEA/PCL and 22 ± 7% for free AEA versus 45 ± 5% or 42 ± 4%; P <0.05 or P <0.01 of control or PCL group, respectively. Likewise, in 10 µM concentration of AEA it was found an iNOS level rise (Fig. 8) with values of 2.50 ± 0.25% for Nps-AEA/PCL and 5 ± 1% for free AEA versus 1.00 ± 0.03% or 1.05 ± 0.03%; P <0.01 or P <0.001 of control or PCL group, respectively. The concentration of nitrites (Fig. 9) was of 120 ± 25% for Nps-AEA/PCL and 250 ± 50% for free AEA versus 50 ± 10% or 60 ± 10%; P <0.01 or P <0.001 of control or PCL group, respectively. The Na^+/K^+ ATPase activity (Fig. 10) was of 20 ± 8% for Nps-AEA/PCL and 5 ± 2% for free AEA versus 45 ± 5% or 42 ± 4%; P <0.01 or P <0.001 of control or PCL group, respectively. Of special interest, these studies show a remarkable difference between AEA encapsulated and non-encapsulated in PCL matrix related to its ability for increasing iNOS expression and NO production and decreasing Na^+/K^+ ATPase activity. This phenomenon could be because the AEA release from Nps would depend on the erosion and dissolution of the PCL matrix. Therefore, it would be carried out in a gradual and controlled manner compared to the treatment with AEA in free form.

3.7 Cytotoxicity study for Nps-AEA/PCL

As shown in Fig. 11*a*, in none of those treatments, applied changes in viability were observed; and in the same way, as seen in Fig. 11*b*, after 24 h of treatment the difference in cell morphology was minimal, and no significant changes were evidenced.

4 Discussion

The results of the present study show in an unprecedented way the satisfactory obtaining of Nps-AEA/PCL by means of the electrospraying technique, whose physical–chemical properties were related to its thermal stability, dimensions, biologicals activity and drug–polymer interactions.

Regarding the results of the thermal analysis performed on the Nps-AEA/PCL, it was observed that the melting temperature of AEA was shifted to lower values with respect to the melting point reported by Aberturas *et al.* [18]. On the other hand, the melting point in the polymer agrees with bibliographic data [27, 28]. The absence of any additional signal in the thermal curve of the Nps-AEA/PCL would indicate this effectively encapsulated in them [29]. The DSC analysis showed an increase in the thermal stability of AEA in the Nps-AEA/PCL with respect to free AEA, in agreement with that reported for other PCL-based nanocomposites [30], which would be a highly desired effect in the development of this type of formulations.

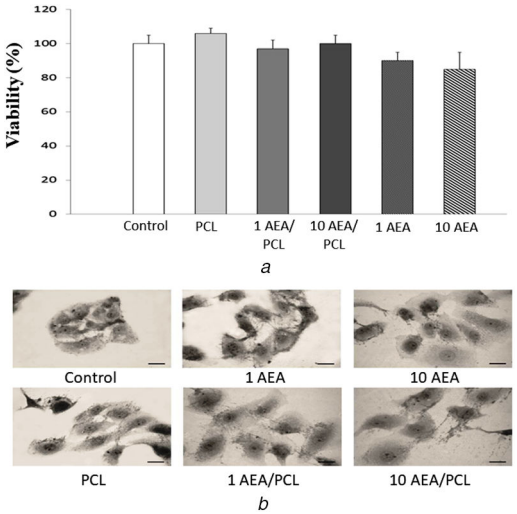

Fig. 11 *MTT assay*
(a) Cell viability, ***(b)*** Cell morphology

Furthermore, FTIR spectroscopy has been used as a powerful tool for the characterisation of nanoparticles [31, 32]. Specifically, as outstanding data, our study proved the existence of drug–polymer interactions that were also observed in other nanoparticulate systems based on PCL [33]. This is another unpublished data of our work since it is known that other studies have reported that PCL does not always establish this type of interaction with the drug that it is incorporated in similar nanostructures [34, 35]. The changes observed between the UV-Vis spectra of free AEA and the Nps-AEA/PCL would also indicate the interaction between both components, since other authors have shown that no bathochromic displacements were observed in the UV–vis spectra of drugs and polymers that do not interact with each other at the nanoscale [36]. This fact would suggest the successful encapsulation of AEA in the Nps-AEA/PCL [37], consistent with our current results obtained from DSC analysis.

Unprecedentedly – and from the exhaustive search in the most current literature – the finding emerges that our study is the first to show the development of AEA/PCL nanoparticles by the electrospraying technique. Other authors have achieved to synthesise this same type of nanoparticles but using the nanoprecipitation method [18, 19]. In general – compared to other processes for obtaining nanoparticles – electrospraying offers essential advantages like better control of the characteristics of these nanostructures due to a large number of variables that can be modified by this technique. Electrospraying can achieve a uniform dispersion of the drug within the polymer matrix with minimal loss of the drug [38]. The ease of operation (one-step process) and profitability are other attractive features of these processes. Furthermore, the direct obtaining of the product in the solid-state eliminates an additional drying step, decreasing the appearance of problems related to the stability of the particles [39]. Despite the large particle size and polydispersity are usually considered a disadvantage of electrospraying, we think that this aspect could be used to obtain a longer duration of the drug release. It is because small particles which exhibit a large surface area would undergo disintegration of their matrix and release of the drug in a first stage, while larger size particles would go through the same process in a longer period of time, extending the therapeutic function of the nanoparticulated formulation. Future studies of in vitro release should be performed to prove this fact, but we considered that this goes beyond the objectives of this work.

The structural analysis by electronic microscopy allowed us to characterise size and shape, but also allowed to identify the presence of particle agglomerates in the SEM image. These formations could be related to temporary blockages of the needle through which the polymer solution circulates and/or the inherent unctuous consistency of the endocannabinoid. Additionally, we consider as another frequent cause of the formation of agglomerates, the absence of stabilising agents such as surfactants or emulsifiers in the formulation of the polymer solution used to obtain the Nps-AEA/PCL [40]. However, and as verified in the physical, chemical and biological tests, these agglomerates did not affect the results.

As for the physicochemical stability of AEA, it is known that because it is a derivative of arachidonic acid it is highly susceptible to oxidative thermal degradation. Of interest, FTIR has been used by other authors to evaluate this possible degradation on arachidonic acid [41]. That is why AEA has a storage temperature of −20°C. In this sense, it results particularly remarkable that the stability tests carried out on the Nps-AEA/PCL showed that AEA is stable even at temperatures of 40°C during a period of 4 months. This result suggests that our formulation of Nps-AEA/PCL would represent a useful option to stabilise an active ingredient labile as AEA, facilitating, in turn, the preservation conditions of this novel pharmaceutical formulation.

In addition to the physicochemical characterisation of the Nps-AEA/PCL obtained, we carried out in vitro biological activity tests as the quantification of iNOS expression in human proximal tubular epithelial cells. It is known that this inducible isoform of

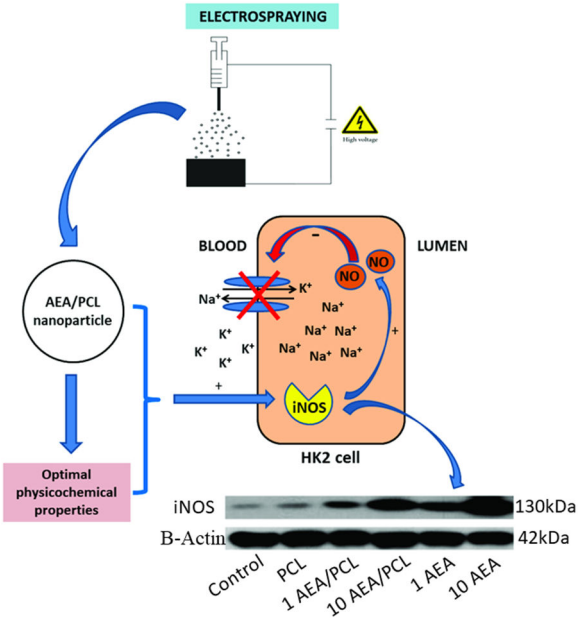

Fig. 12 *Graphical abstract*

NOS is widely expressed in cells of the renal proximal tubule [42]. To highlight, several studies have reported on a promising antihypertensive effect (primarily vasodilator) of AEA mediated by NO release in different cell types [43–45]. Nevertheless, the aforementioned effect, specifically related to renal ion transport, currently has not been demonstrated through the administration of AEA encapsulated in polymeric nanoparticles. In fact, unpublished, our results would demonstrate for the first time that the Nps-AEA/PCL were able to increase in a dose-dependent manner the expression of iNOS in HK2 cells, with the consequent increase in NO production by these cells. In order to complement the findings, we also decided to evaluate the effect of Nps-AEA/PCL on Na^+/K^+ ATPase activity. In this sense, we demonstrated a dose-dependent decrease in Na^+/K^+ ATPase activity, confirming our initial hypothesis. Finally, although it is known that in some circumstances the NO derived from iNOS is an important mediator of the apoptosis of tubular epithelial cells induced by macrophages in vitro [46], we demonstrated that at the concentrations produced in our work no cytotoxicity was observed. This aspect constitutes one more point in favour of the use of AEA, especially encapsulated in Nps, in order to modulate the activity of the Na^+/K^+ ATPase in HK2 cells.

5 Conclusions

The use of biocompatible, biodegradable and non-toxic organic polymers such as PCL would allow the development of new pharmaceutical formulations for the controlled/prolonged release of various types of active ingredients with attractive pharmacological properties such as AEA but dismissed for their physicochemical and pharmacokinetic limitations and disadvantages. Our study demonstrated synthesis efficiency and stability of this compound, also proved the ability of Nps-AEA/PCL to decrease Na^+/K^+ ATPase activity at the renal level in a mechanism that could be related to the iNOS expression and NO levels (Fig. 12 or graphical abstract). Future in vivo studies should be performed to demonstrate the usefulness of Nps-AEA/PCL in cardiovascular pathologies treatment such as arterial hypertension and other related diseases.

Finally, the strategies of active targeting (decoration of Nps surface with ligands for specific receptors), passive targeting (regulation of the Nps size and surface properties) or physical targeting (using physical forces such as the application of a magnetic field to guide Nps) are of special interest when designing new nanoparticulate systems for drug delivery. In this sense, different pharmacological targeting strategies could be used in the future to achieve the specific localisation of these Nps-AEA/PCL in sites of interest such as the kidneys or other cardiovascular organs.

6 Acknowledgments

The author(s) disclosed receipt of the following financial support for the research, authorship, and/or publication of this article: This work was supported by grants from the Research and Technology Council of Cuyo University (SECyT), Mendoza, Argentina, and from the National Council of Scientific and Grant PICT 2016-4541, both of which were granted to Walter Manucha. V.M.M.G and M.G.R, thanks for fellowships to CONICET. G.E.N is member of CIC-CONICET. The authors thank for financial support to PIP-CONICET 912 and PROICO 2-2016, SECyT-UNSL, San Luis, Argentina.

7 References

[1] Ngwa, W., Kumar, R., Moreau, M., *et al.*: 'Nanoparticle drones to target lung cancer with radiosensitizers and cannabinoids', *Front. Oncol.*, 2017, **7**, p. 208

[2] Hernán Pérez de la Ossa, D., Gil-Alegre, M.E., Ligresti, A., *et al.*: 'Preparation and characterization of Δ(9)-tetrahydrocannabinol-loaded biodegradable polymericmicroparticles and their antitumoral efficacy on cancer cell lines', *J. Drug Target.*, 2013, **21**, pp. 710–718

[3] Hernán Pérez de la Ossa, D., Ligresti, A., Gil-Alegre, M.E., *et al.*: 'Poly-ε-caprolactone microspheres as a drug delivery system for cannabinoid administration: development, characterization and in vitro evaluation of their antitumoral efficacy', *J. Controlled Release*, 2012, **161**, pp. 927–932

[4] Stanley, C., O'Sullivan, S.E.: 'Vascular targets for cannabinoids: animal and human studies', *Br. J. Pharmacol.*, 2014, **171**, pp. 1361–1378

[5] Conte, R., Marturano, V., Peluso, G., *et al.*: 'Recent advances in nanoparticle-mediated delivery of anti-inflammatory phytocompounds', *Int. J. Mol. Sci.*, 2017, **18**, p. E709

[6] Esposito, E., Drechsler, M., Cortesi, R., *et al.*: 'Encapsulation of cannabinoid drugs in nanostructured lipid carriers', *Eur. J. Pharm. Biopharm.*, 2016, **102**, pp. 87–91

[7] Esposito, E., Ravani, L., Drechsler, M., *et al.*: 'Cannabinoid antagonist in nanostructured lipid carriers (NLCs): design, characterization and in vivo study', *Mater. Sci. Eng. C, Mater. Biol. Appl.*, 2015, **48**, pp. 328–336

[8] Punyamurthula, N.S., Adelli, G.R., Gul, W., *et al.*: 'Ocular disposition of Δ8-tetrahydrocannabinol from various topical ophthalmic formulations', *AAPS Pharm. Sci. Tech.*, 2017, **18**, pp. 1936–1945

[9] Nouar, A.: 'Cannabinoid encapsulating nanoparticles for atherosclerosis therapy. An in vitro study [master's thesis]'. Delft University of Technology, the Netherlands, 2017

[10] Grottkau, B.E., Cai, X., Wang, J., *et al.*: 'Polymeric nanoparticles for a drug delivery system', *Curr. Drug Metab.*, 2013, **14**, pp. 840–846

[11] Martín-Banderas, L., Muñoz-Rubio, I., Prados, J., *et al.*: 'In vitro and in vivo evaluation of Δ^9-tetrahidrocannabinol/PLGA nanoparticles for cancer chemotherapy', *Int. J. Pharm.*, 2015, **487**, pp. 205–212

[12] Martín-Banderas, L., Muñoz-Rubio, I., Álvarez-Fuentes, J., *et al.*: 'Engineering of Δ9-tetrahydrocannabinol delivery systems based on surface modified-PLGA nanoplatforms', *Colloids Surf. B. Biointerfaces*, 2014, **123**, pp. 114–122

[13] Hernán Pérez de la Ossa, D., Lorente, M., Gil-Alegre, M.E., *et al.*: 'Local delivery of cannabinoid-loaded microparticles inhibits tumor growth in a murine xenograft model of glioblastoma multiforme', *PLoS One*, 2013, **8**, (1), p. e54795

[14] Durán-Lobato, M., Muñoz-Rubio, I., Holgado, M.A., *et al.*: 'Enhanced cellular uptake and biodistribution of a synthetic cannabinoid loaded in surface-modified poly(lactic-co-glycolic acid) nanoparticles', *J. Biomed. Nanotechnol.*, 2014, **10**, pp. 1068–1079

[15] Martín-Banderas, L., Alvarez-Fuentes, J., Durán-Lobato, M., *et al.*: 'Cannabinoid derivate-loaded PLGA nanocarriers for oral administration: formulation, characterization, and cytotoxicity studies', *Int. J. Nanomed.*, 2012, **7**, pp. 5793–5806

[16] Berrocoso, E., Rey-Brea, R., Fernández-Arévalo, M., *et al.*: 'Single oral dose of cannabinoid derivate loaded PLGA nanocarriers relieves neuropathic pain for eleven days', *Nanomedicine*, 2017, **13**, pp. 2623–2632

[17] Xian, S., Parayath, N.N., Nehoff, H., *et al.*: 'The use of styrene maleic acid nanomicelles encapsulating the synthetic cannabinoid analog WIN55,212-2 for the treatment of cancer', *Anticancer Res.*, 2015, **35**, pp. 4707–4712

[18] Aberturas, M.R., Hernán Pérez de la Ossa, D., Gil, M.E., *et al.*: 'Anandamide-loaded nanoparticles: preparation and characterization', *J. Microencapsul.*, 2011, **28**, pp. 200–210

[19] Ligresti, A., De Petrocellis, L., Hernán Pérez de la Ossa, D., *et al.*: 'Exploiting nanotechnologies and TRPV1 channels to investigate the putative anandamide membrane transporter', *PLoS One*, 2010, **5**, p. e10239

[20] Pawar, A., Thakkar, S., Misra, M.: 'A bird's eye view of nanoparticles prepared by electrospraying: advancements in drug delivery field', *J. Controlled Release*, 2018, **286**, pp. 179–200

[21] Silva, G.B., Atchison, D.K., Juncos, L.I., *et al.*: 'Anandamide inhibits transport-related oxygen consumption in the loop of Henle by activating CB1 receptors', *Am. J. Physiol. Renal Physiol.*, 2013, **304**, pp. 376–381

[22] Jenkin, K.A., McAinch, A.J., Grinfeld, E., *et al.*: 'Role for cannabinoid receptors in human proximal tubular hypertrophy', *Cell. Physiol. Biochem.*, 2010, **26**, pp. 879–886

[23] Sampaio, L.S., Taveira Da Silva, R., Lima, D., *et al.*: 'The endocannabinoid system in renal cells: regulation of Na(+) transport by CB1 receptors through distinct cell signalling pathways', *Br. J. Pharmacol.*, 2015, **172**, pp. 4615–4625
[24] Griess, J.O.: 'On a new series of in which nitrogen is substituted for hydrogen', *Philos. Trans. Royal Soc. B*, 1864, **154**, pp. 667–731
[25] Jiang, M., Sheetz, M.: 'Cargo-activated ATPase activity of kinesin', *Biophys. J.*, 1995, **68**, pp. 15–16
[26] Jaiswal, M., Dinda, A.K., Gupta, A., *et al.*: 'Polycaprolactone diacrylate crosslinked biodegradable semi-interpenetrating networks of polyacrylamide and gelatin for controlled drug delivery', *Biomed. Mater.*, 2010, **5**, (6), p. 065014
[27] Kweon, H.Y., Yoo, M.K., Park, I.K.: 'A novel degradable polycaprolactone networks for tissue engineering', *Biomater.*, 2003, **24**, pp. 801–808
[28] Ramírez-Agudelo, R., Scheuermann, K., Gala-García, A., *et al.*: 'Hybrid nanofibers based on poly-caprolactone/gelatin/hydroxyapatite nanoparticles-loaded doxycycline: effective anti-tumoral and antibacterial activity', *Mater. Sci. Eng. C, Mater. Biol. Appl.*, 2018, **83**, pp. 25–34
[29] Radhakrishnan, S., Seeram, R.: 'Electrosprayed nanoparticles for drug delivery and pharmaceutical applications', *Biomatter*, 2013, **3**, p. e24281
[30] Khandanlou, R., Ahmad, M.B., Shameli, K., *et al.*: 'Studies on properties of rice straw/polymer nanocomposites based on polycaprolactone and Fe_3O_4 nanoparticles and evaluation of antibacterial activity', *Int. J. Mol. Sci.*, 2014, **15**, pp. 18466–18483
[31] Biswas, N., Thomas, S., Sarkar, A., *et al.*: 'Adsorption of methimazole on silver nanoparticles: FTIR, Raman, and surface-enhanced Raman scattering study aided by density functional theory', *J. Phys. Chem.*, 2009, **113**, pp. 7091–7100
[32] Sarmento, B., Ferreira, D., Veiga, F., *et al.*: 'Characterization of insuline-loaded alginate nanoparticles produced by ionotropic pre-gelation through DSC and FTIR studies', *Carbohydr. Polym.*, 2006, **66**, pp. 1–7
[33] Danafar, H.: 'MPEG-PCL copolymeric nanoparticles in drug delivery systems', *Cogent Med.*, 2016, **3**, p. 1142411
[34] Mady, F.M., Shaker, M.A.: 'Enhanced anticancer activity and oral bioavailability of ellagic acid through encapsulation in biodegradable polymeric nanoparticles', *Int. J. Nanomed.*, 2017, **12**, pp. 7405–7417
[35] Sathyamoorthy, N., Magharla, D., Chintamaneni, P., *et al.*: 'Optimization of paclitaxel loaded poly (ε-caprolactone) nanoparticles using box Behnken design', *BJBAS*, 2017, **6**, pp. 362–373
[36] Kalita, S., Devi, B., Kandimalla, R., *et al.*: 'Chloramphenicol encapsulated in poly-ε-caprolactone-pluronic composite: nanoparticles for treatment of MRSA-infected burn wounds', *Int. J. Nanomed.*, 2015, **10**, pp. 2971–2984
[37] El-Houssiny, A.S., Ward, A.A., Mostafa, D.M., *et al.*: 'Drug-polymer interaction between glucosamine sulfate and alginate nanoparticles: FTIR, DSC and dielectric spectroscopy studies', *ANSN*, 2016, **7**, p. 025014
[38] Husain, O., Lau, W., Edirisinghe, M., *et al.*: 'Investigating the particle to fibre transition threshold during electrohydrodynamic atomization of a polymer solution', *Mater. Sci. Eng. C, Mater. Biol. Appl.*, 2016, **65**, pp. 240–250
[39] Sridhar, R., Ramakrishna, S.: 'Electrosprayed nanoparticles for drug delivery and pharmaceutical applications', *Biomatter*, 2013, **3**, p. e24281
[40] Mielke, J., Dohányosová, P., Müller, P., *et al.*: 'Evaluation of electrospray as a sample preparation tool for electron microscopic investigations: toward quantitative evaluation of nanoparticles', *Microsc. Microanal.*, 2017, **23**, pp. 163–172
[41] Gocen, T., Bayari, S.H., Guven, M.H.: 'Conformational and vibrational studies of arachidonic acid, light and temperature effects on ATR-FTIR spectra', *Spectrochim, Acta A, Mol. Biomol. Spectrosc.*, 2018, **203**, pp. 263–272
[42] Satoh, N., Nakamura, M., Suzuki, A., *et al.*: 'Effects of nitric oxide on renal proximal tubular Na + transport', *BioMed Res. Int.*, 2017, p. 6871081
[43] Stanley, C.P., Hind, W.H., Tufarelli, C., *et al.*: 'The endocannabinoid anandamide causes endothelium-dependent vasorelaxation in human mesenteric arteries', *Pharmacol. Res.*, 2016, **113**, pp. 356–363
[44] Baranowska-Kuczko, M., Kozłowska, H., Kozłowski, M.: 'Mechanisms of endothelium-dependent relaxation evoked by anandamide in isolated human pulmonary arteries', *Naunyn Schmiedebergs Arch. Pharmacol.*, 2014, **387**, pp. 477–486
[45] Lobato, N.S., Filgueira, F.P., Prakash, R.: 'Reduced endothelium-dependent relaxation to anandamide in mesenteric arteries from young obese Zucker rats', *PLoS One*, 2013, **8**, p. e63449
[46] Kipari, T., Cailhier, J.F., Ferenbach, D.: 'Nitric oxide is an important mediator of renal tubular epithelial cell death in vitro and in murine experimental hydronephrosis', *Am. J. Pathol.*, 2006, **169**, (2), pp. 388–399